IEEE Access
Multidisciplinary ⋮ Rapid Review ⋮ Open Access Journal

Received October 22, 2019, accepted November 5, 2019, date of publication November 12, 2019,
date of current version December 10, 2019.

Digital Object Identifier 10.1109/ACCESS.2019.2953048

Deep Belief Network-Based Gas Path Fault Diagnosis for Turbofan Engines

JIANGUO XU[1], XINGYI LIU[1], BINBIN WANG[1], AND JIAQI LIN[2]
[1]College of Energy and Power Engineering, Nanjing University of Aeronautics and Astronautics, Nanjing 210016, China
[2]China Mobile (Suzhou) Software Technology Company Ltd., Suzhou 215000, China

Corresponding author: Jianguo Xu (xujianguo@nuaa.edu.cn)

This work was supported in part by the China Postgraduate Research and Practice Innovation Program of Jiangsu Province under Grant SJCX18_0097.

ABSTRACT A gas path fault diagnosis scheme for turborfan engines based on deep belief network (DBN) is presented. The scheme is constructed according to the diagnosis principles of gas path faults and is composed of a turbofan engine reference model and a DBN diagnosis model. The DBN diagnosis model is a stacked network of several restricted Boltzmann machines (RBM) and was trained with the contrastive divergence algorithm and the back propagation algorithm. To optimize the DBN performance, the orthogonal tests L_{25} (5^7) were adopted to determine the hyper-parameters, such as learning rate, hidden layer number, hidden layer neuron number, etc. The proposed DBN-based scheme was applied to diagnose the gas path faults of a turbofan engine model and compared with BP-based and SVM-based schemes. The results show that the fault diagnosis accuracy of the DBN-based scheme is as high as 96.59%, and the DBN-based scheme has dramatic performance advantages over the other two schemes.

INDEX TERMS Turbofan engine, gas path, fault diagnosis, deep belief network, orthogonal test.

I. INTRODUCTION

The turbofan engine is the main propulsion system for commercial and military aircrafts. It is a safety critical system and its performance directly affects the reliability and safety of aircrafts. Gas turbine engine faults are mainly divided into three categories: gas path faults, structural faults and sensor/actuator faults. Gas path components usually work under harsh temperature, speed and stress conditions. Furthermore, they are affected by the problems of erosion, corruption and foreign object damage. Therefore, gas path components are prone to performance deterioration, and their faults account for a large proportion of turbofan engine faults. We study the gas path fault diagnosis method for turbofan engines in this paper.

At present, the main difficulties of gas path fault diagnosis are as follows [1]–[6]:

1) The measurable parameter number of turbofan engines is less than the unmeasurable parameter number.
2) There is a strong correlation between different turbofan engine faults, and it is difficult to distinguish similar turbofan engine faults.
3) There may be measurement noise in measurement signals.
4) There is strong nonlinearity, uncertainty and complexity in turbofan engine behavior, and the working environment conditions tend to change with respect to time.

Because neural network (NN) has great advantages in dealing with nonlinear problems and modeling complex and nonlinear systems, it has been introduced to the field of aero-engine fault diagnosis by many experts and scholars. M. Zedda *et al.* proposed a NN-based diagnostic system for a low by-pass ratio turbofan engine and found that the system can quantify multiple faults affecting the engine components by using few and noisy measurements [7]. S. O. T. Ogaji *et al.* applied multiple NNs method to diagnose and quantify single and dual-sensor faults in a two shaft stationary gas-turbine [8]. On the basis of a bank of eight dynamic NNs, S. Sina Tayarani-Bathaie *et al.* proposed a fault detection and isolation scheme, which can detect different component faults for a dual spool turbofan engine in the steady state [9]. However, conventional NNs' generalization ability is not good and they are prone to converge to local optimal solutions.

Deep learning is a branch of machine learning which allows computational models that are composed of multiple

The associate editor coordinating the review of this manuscript and approving it for publication was Venkateshkumar Mohan.

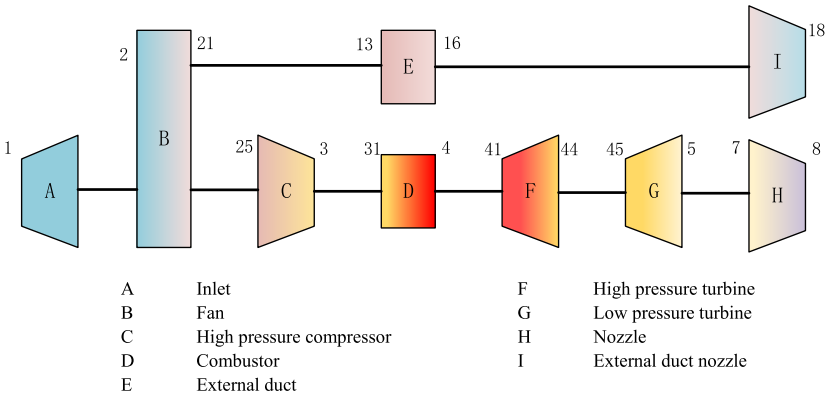

FIGURE 1. Schematic of turbofan engine gas path components.

processing layers to learn representations of data with multiple levels of abstraction [10]. Recently, deep learning has been adopted in various areas such as computer vision, automatic speech recognition, natural language processing, audio recognition and bioinformatics, and has achieved significant achievements. As a result, deep learning has also aroused great attentions in the field of fault diagnosis, and is getting more and more research and application [11]–[12].

Deep learning models are the development of conventional NNs and include several variants such as auto-encoders, DBNs, convolutional neural networks, recurrent neural networks and so on. DBN is a probabilistic generation model, which generates a joint distribution of observed data and labels compared with the traditional discriminant models. To overcome the shortcomings of NNs, some researchers tried to use DBN as the diagnosis tool for aero-engines. P. Tamilselvan *et al.* proposed a multi-sensory DBN-based health state classification model, which was verified in benchmark classification problems as well as in aircraft engine health diagnosis [13]. X. Lin *et al.* presented a DBN-based algorithm (ad_DBN) to improve the malfunction diagnosis accuracy of rotating components in an aeronautical turboshaft engine [14]. Although DBN has achieved excellent performance in many classification and feature extraction applications, it has several hyper-parameters to be determined, which have great influence on the DBN performance.

To investigate the influence of different hyper-parameters on DBN performance and find the best combination of hyper-parameters, the orthogonal test method can be chosen as a suitable tool. The method is a statistical technique to arrange tests and data analysis with an orthogonal table, which selects a suitable number of representative test cases from many test data, that have evenly dispersed, neat comparable characteristics [15]. By applying the orthogonal test method, the test times can be reduced and the optimized parameters can be found quickly. Z. Li *et al.* proposed a wavelet-NN diagnosis system for a vibrating screen, and the system parameters were optimized through orthogonal tests [16]. D. J. Cai et al. optimized the operating conditions of the extraction of flavonoid from Fructus Gardeniae by employing orthogonal tests L9 (34) [17].

In light of the above research work, a DBN-based fault diagnosis scheme for the gas path components of turbofan engines is proposed in this paper. Based on the analysis of the diagnosis principles of gas path faults, the scheme is constructed with a turbofan engine reference model and a DBN diagnosis model. The turbofan engine reference model is a component-level engine model. And the DBN diagnosis model is constructed by stacking multiple RBMs, and then adding a full connection layer as the output layer. Furthermore, the DBN model was trained with the contrastive divergence pre-training algorithm and the back propagation fine-tuning algorithm. And the model hyper-parameters were optimized through the seven-factor and five-level orthogonal tests L25 (5^7). In the end, the simulation experiments were carried out to evaluate the diagnosis performance of the DBN-based scheme, compared with BP-based and SVM-based schemes. The results indicate that the scheme has high diagnosis accuracy and can be used to find early anomalies and faults for condition-based maintenance, thus reducing maintenance costs.

The remainder of this paper is organized as follows. In Section 2, the DBN-based fault diagnosis scheme for the gas path components of turbofan engines are described. In Section 3, the structure of the DBN diagnosis model and the hyper-parameter optimization method are presented and described in detail. Simulation results and the performance comparison with other AI methods are presented in Section 4, followed by the conclusions in Section 5.

II. DBN-BASED FAULT DIAGNOSIS SCHEME

For turbofan engines with large bypass ratio, its gas path components include a fan, a high pressure compressor, a combustor, a high pressure turbine, a low pressure turbine, and so on, as illustrated in Fig. 1. The engine station numbers are as follows:

1 Inlet entry,
13 External duct entry,
16 External duct exit/ External duct nozzle entry,
18 External duct nozzle exit,
2 Inlet exit/Fan entry,

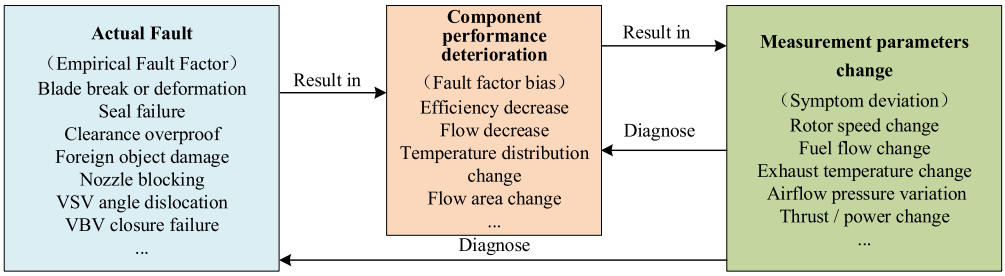

FIGURE 2. Principle diagram of engine fault diagnosis.

21 Fan exit,
25 High pressure compressor entry,
3 High pressure compressor exit,
31 Combustor entry,
4 Combustor exit,
41 High pressure turbine entry,
44 High pressure turbine exit,
45 Low pressure turbine entry,
5 Low pressure turbine exit,
7 Nozzle entry,
8 cNozzle exit.

Although the weight of these components only constitutes a small part of the whole engine weight, their maintenance cost accounts for 60% of the total maintenance cost. Furthermore, their faults usually account for about 90% of the engine faults. So the reliability of gas path components is of great importance for the whole engine [18], [19].

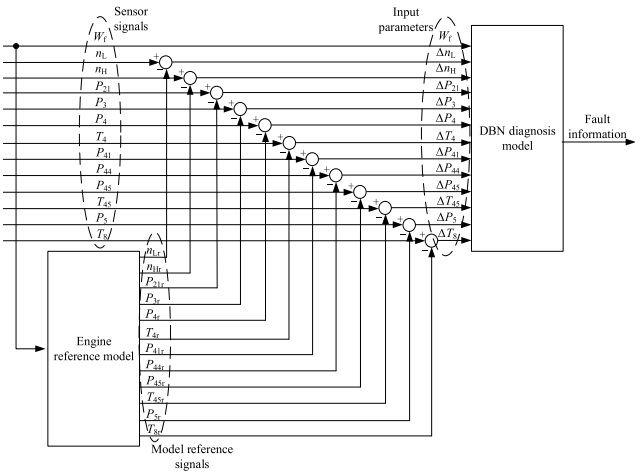

FIGURE 3. DBN-based fault diagnosis scheme for turbo-fan engines.

A. FAULT DIAGNOSIS PRINCIPLE

Compressor increases air pressure through high-speed rotating impellers. When the compressor performance changes, its efficiency will change accordingly. Therefore, the compressor efficiency can be used as the criteria for compressor fault diagnosis.

The faults of combustor are mainly caused by the faults of fuel control system, such as integrated controller failure, sensor indication distortion, fuel supply regulator components block, fuel supply pressure fluctuation, leakage at seal, fuel nozzle block, insufficient fuel pressure, etc., which all show the decline of combustion efficiency.

The high/low pressure turbines convert the energy of gas flow into mechanical energy. Turbine blades are directly impacted by high temperature and high pressure gas flow, so the failure rate of turbines is very high. When the turbines fail, their isentropic efficiency decreases and the performance of the whole engine also decreases.

As illustrated in Fig. 2, the actual faults of the engine (such as blade breakage or deformation, etc.) result in the performance deterioration of the components, which leads to the changes of the measurement parameters. If the above process is regarded as a positive process, then the fault diagnosis is its reverse process. There are two kinds of engine fault diagnosis. Firstly, according to the changes of the engine measurement parameters to determine the performance of the engine components, so as to achieve fault location. Secondly, the physical faults of the engine can be directly judged by the changes of the measurement parameters [20]–[21]. The proposed fault diagnosis scheme in this paper belongs to the former.

B. FAULT DIAGNOSIS SCHEME

The DBN-based fault diagnosis scheme is shown Fig. 3.

As shown in Fig.3, the fault diagnosis scheme is comprised of an engine reference model and a DBN diagnosis model. And here the engine reference model is a component-level turbo-fan engine model.

Thirteen measurable variables are selected for fault diagnosis, including fuel flow W_f, low pressure spool speed n_L, high pressure spool speed n_H, total pressure after fan P_{21}, total pressure after high pressure compressor P_3, total temperature and total pressure after combustion chamber T_4, P_4, total pressure before high pressure turbine P_{41}, total pressure after high pressure turbine P_{44}, total temperature and total pressure before low pressure turbine T_{45}, P_{45}, total pressure after low pressure turbine P_5, and total temperature after nozzle T_8. The difference between these sensor signals and the output parameters of the engine reference model is calculated, and the results are used as the input of the DBN diagnosis model.

TABLE 1. Five typical fault modes and healthy mode of gas path components.

Fault type	Fault cause	Diagnostic label
F00	Healthy mode	[1, 0, 0, 0, 0, 0]
F01	Fan efficiency deterioration	[0, 1, 0, 0, 0, 0]
F02	Efficiency deterioration of high pressure compressor	[0, 0, 1, 0, 0, 0]
F03	Combustor efficiency deterioration	[0, 0, 0, 1, 0, 0]
F04	Efficiency deterioration of high pressure turbine	[0, 0, 0, 0, 1, 0]
F05	Efficiency deterioration of low pressure turbine	[0, 0, 0, 0, 0, 1]

The DBN model outputs six working modes, including five fault modes and a healthy mode. The five fault modes are described in detail in the next subsection.

C. FAULT CLASSIFICATION

According to the deterioration degree of performance, gas path faults can be divided into two categories, component performance degradation and component fault. Generally speaking, when the engine components work in high temperature and high pressure for a long time, the component performance will deteriorate to some extent. The deterioration is generally characterized by the variation of the performance parameters of components (fans, compressors, combustors, turbines, etc.), which are called the gas path health parameters. The serious deterioration of the health parameters denotes the faults of the gas path components.

The objective of this research is the fault diagnosis of a two-shaft turbofan engine with high bypass ratio. Its main gas path components include inlet, fan, high pressure compressor, combustor, high pressure turbine, low pressure turbine, nozzle, external duct, external duct nozzle, etc. Five typical fault modes of gas path are studied in this paper, fan fault, high pressure compressor fault, combustor fault, high pressure turbine fault and low pressure turbine fault, as listed in Table 1.

III. DBN DIAGNOSIS MODEL

Deep Belief Network [22] is a deep neural network proposed by Geoffrey E. Hinton in 2006. Because DBN has a probability framework with multiple (greater than or equal to 2) hidden layers, it can learn representations of data through multiple levels of abstraction, and it has better feature extraction ability and classification ability compared with conventional machine learning algorithms, such as backpropagation neural network (BP) and support vector machine (SVM). In this paper, based on DBN and tensorflow platform [23], the gas path fault diagnosis approach for turbofan engines is studied. Fig. 4 shows the training and test flow chart of the diagnosis model.

A. STRUCTURE OF DBN MODEL

DBN is a probabilistic generation model, which generates a joint distribution of observed data and labels compared with the traditional discriminant models. DBN is constructed by stacking multiple RBMs, and then adding a full connection

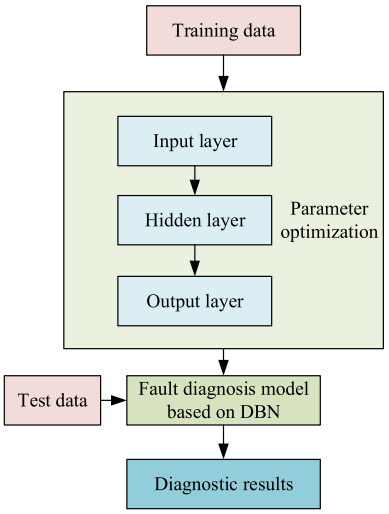

FIGURE 4. Training and test flow chart of DBN diagnosis model.

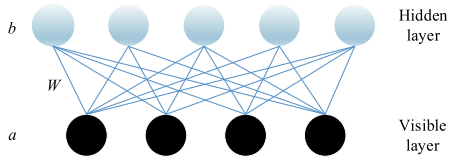

FIGURE 5 RBM structure diagram

FIGURE 5. RBM structure diagram.

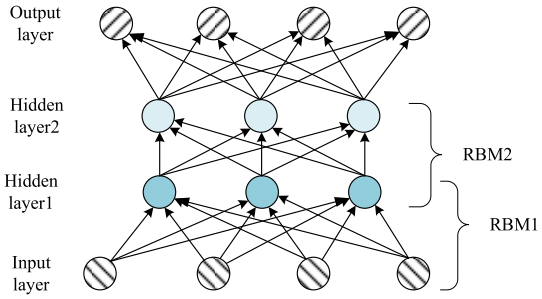

FIGURE 6. Structure of a typical DBN.

layer as the output layer according to application requirements. Fig. 5 shows a typical RBM structure, and Fig. 6 shows the structure of a typical DBN with two RBMs [24].

The RBM consists of two layers of neurons, one visible layer and one hidden layer. Each neuron is a binary neuron, with only two values: 0 and 1. Value 1 indicates that the neuron is active and value 0 indicates the neuron inactive. The two layers are fully connected, and there is no connection between neurons in the same layer.

The energy function E is defined as following [25], [26]:

$$E(v, h|\theta) = -\sum_{i=1}^{n} a_i v_i - \sum_{j=1}^{m} b_j h_j - \sum_{i=1}^{n}\sum_{j=1}^{m} v_i w_{ij} h_j \quad (1)$$

In (1), where $\theta = \{W, a, b\}$ are the model parameters, i and j are the indexes of visible and hidden neurons, respectively.

a_i is the bias of the i th visible neuron, and b_j is the bias of the jth hidden neuron, and w_{ij} is the connection weight between v_i and h_j.

The joint distribution over all visible and hidden neurons is defined as:

$$Z(\theta) = \sum_{v,h} e^{-E(v,h|\theta)}$$
$$P(v, h|\theta) = \frac{e^{-E(v,h|\theta)}}{Z(\theta)} \tag{2}$$

The condition probability that a neuron's value is 1 can be written as:

$$P(h_j = 1|v) = sigmoid(b_j + \sum_i v_i w_{ij})$$
$$P(v_i = 1|h) = sigmoid(a_i + \sum_j h_j w_{ij}^T) \tag{3}$$

where *sigmoid* is the logistic function, which is defined as $sigmoid(x) = 1/(1 + e^{-x})$. The sigmoid function has a good explanation for the activation probability of neurons, from complete inactivation (0) to full saturation activation (1). As a result, it is widely used in many probability models and auto encoder models.

The training of RBM is to estimate the parameters according to the training samples, so that the inferred value of a visible layer neuron can be as close as possible to the real value of it. And the RBM parameters can be estimated by using the maximum likelihood method. The derivate of the log probability of the training data can be computed as follows:

$$-\frac{\partial \ln P(v)}{\partial w_{ij}} = \langle v_i h_j \rangle_{\mathrm{d}} - \langle v_i h_j \rangle_{\mathrm{m}}$$
$$-\frac{\partial \ln P(v)}{\partial b_j} = \langle h_j \rangle_{\mathrm{d}} - \langle h_j \rangle_{\mathrm{m}}$$
$$-\frac{\partial \ln P(v)}{\partial a_i} = \langle v_i \rangle_{\mathrm{d}} - \langle v_i \rangle_{\mathrm{m}} \tag{4}$$

where $\langle \cdot \rangle_{\mathrm{d}}$ denotes an expectation with respect to the data distribution and $\langle \cdot \rangle_{\mathrm{m}}$ is an expectation with respect to the distribution defined by the model. The former term labeled the positive phase increases the probability of training data whilst the latter term dubbed the negative phase decreases the probability of samples generated by the model.

However, the expectation $\langle \cdot \rangle_m$ is intractable to compute. Therefore, in practice, an approximation to the gradient so-called the contrastive divergence (CD) is used. The CD algorithm has become the standard algorithm for training DBN. The training process is divided into two stages. The first stage is a bottom-up unsupervised learning and the second stage is a supervised learning from top to bottom. The specific process is as follows. Firstly, the connection weights W and bias a, b are initialized randomly. Then the input data are assigned to the neurons of the visible layer, and the hidden layer is reconstructed with Gibbs sampling. Thus the connection weights W and bias a, b are optimized repeatedly and all the RBMs are trained sequentially. The second stage is a top-down supervised learning, in which the DBN is further fine-tuned with back propagation (BP) algorithm according to the labels of the training dataset. The whole training process is shown in Fig. 7.

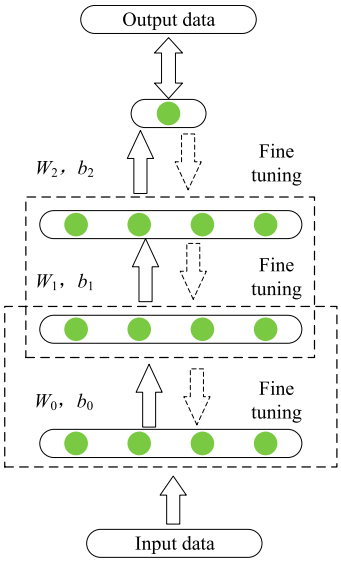

FIGURE 7. DBN training process.

B. TRAINING AND TEST DATASET GENERATION

In this study, a component-level turbofan engine model was used to generate the training and test dataset. The flight altitude was 32,000 feet at cruise altitude, and the flight speed set to 0.7 Mach at cruise speed. The efficiency degradation range of each component was set to [0, 0.1], the degradation step of 0.01 was selected to gradually reduce the efficiency value for different components, and finally the dataset for the engine with different performance was obtained. The threshold value of engine faults was chosen to be 0.05 [27], that is, if the efficiency degradation is greater than or equal to the threshold value, the engine is in fault condition, otherwise, the engine is in healthy working condition. With this method, a dataset of 34,000 samples was obtained, including 14,000 healthy samples (efficiency degradation within threshold) and 20,000 faulty samples (efficiency degradation beyond threshold, 4 fault types and 5000 samples of each type).

In order to ensure the reliability of the diagnosis results, it is necessary to normalize all the input parameters. We adopt the min-max normalization method as shown in (5) [28].

$$x^* = \frac{x - x_{\min}}{x_{\max} - x_{\min}} \tag{5}$$

In (5), $x_{\min}$ and $x_{\max}$ denote the minimum and the maximum of the input parameter x, respectively, and x^* denotes the normalized value of x. Thus the input parameter x is re-scaled within the range [0, 1].

TABLE 2. Orthogonal test design (seven factors and five levels).

Level	Factor						
	Pre-training learning rate	Fine-tuning learning rate	Number of hidden layer's neurons	Hidden layer number	Batch size	Dropout	Momentum
1	0.0001	0.0001	10	2	100	0	0
2	0.0005	0.0005	15	3	500	0.01	0.1
3	0.001	0.001	20	4	1000	0.05	0.2
4	0.005	0.005	25	5	1500	0.1	0.3
5	0.01	0.01	30	6	2000	0.15	0.4

After the normalizing process, the original dataset is divided into one training subset and one test subset. The partition ratio between the training subset and the test subset will affect the fault diagnosis performance to a certain extent. In general, when the training subset becomes larger, the training accuracy of the DBN model may also be higher. But if the test subset is too small, the generalization ability of the DBN model cannot be verified effectively. Based on our experience, it is determined that there are 30,000 samples in the training subset and 4000 samples in the test subset. And all the samples are randomly grouped into the two subsets.

C. HYPER-PARAMETER OPTIMIZATION

When we construct the DBN model for aero-engine fault diagnosis, there are several hyper-parameters need to be determined. These hyper-parameters include learning rate, number of neurons in each hidden layer, number of hidden layers, regularization factor, dropout and so on. They dramatically affect the training effects of the DBN model.

The traditional hyper-parameter selection approach is segmental search, which selects the hyper-parameters according to the training results with different hyper-parameter combinations randomly selected in different segments. The approach is not a good choice when the hyper-parameter number increases.

To optimize the DBN hyper-parameters, the orthogonal tests L_{25} (5^7) were used and the test conditions are shown in Table 2. The seven factors are pre-training learning rate, fine-tuning learning rates, number of hidden layer's neurons, hidden layer number, batch size, dropout and momentum. Every factor has five levels to be optimized. So twenty-five tests were carried out when the pre-training learning rates and the fine-tuning learning rate were 0.0001, 0.0005, 0.001, 0.005 and 0.01, the numbers of the hidden layer neurons were 10, 15, 20, 25 and 30, the hidden layer numbers were 2, 3, 4, 5 and 6, the dropouts were 0, 0.01, 0.05, 0.1 and 0.15, and the momentums were 0, 0.1, 0.2, 0.3 and 0.4.

Table 3 is the results of the orthogonal tests and the extreme difference analysis. Every diagnosis accuracy is the average of 10 diagnosis results. Furthermore, an orthogonal analysis was carried out. As shown in Table 3, K i was obtained by adding any number of columns corresponding to i factor, and ki is the average accuracy of the same factor in different levels. R is the difference between the maximum value and the minimum value of k i of any columns. As seen in Table 3, the hidden layer number is found to be the most important factor. The best diagnosis accuracy is obtained when the hidden layer number is 3, the pre-training learning rate is 0.0005, the fine-tuning learning rate is 0.005 and the number of hidden layer neurons is 25, etc.

According to the results of Table 3, the diagnosis accuracy trend chart of each factor was drawn in Fig. 8. It can be found that the learning rate between 0.0001 and 0.0005 is more appropriate because large learning rate may cause the global optimum to be skipped in the training process. It also can be seen that the DBN models with more hidden layers do not necessarily have better performance and the accuracy of the 2-hidden-layer DBN model is the best. And the optimal range of hidden layer neuron number is between 20 and 25.

In the end, according to the diagnosis accuracy trend chart in Fig. 8, all the hyper-parameters were decided as shown in Table 4. The structure of the optimized DBN model is shown in Fig. 9. There are four layers in the DBN model. The neurons in the input layer correspond to the 13 measurement parameters. The neuron numbers in both hidden layers are 20. And the six neurons in the output layer correspond to one healthy mode and five gas path fault modes.

Through the above analysis and calculation, we can see that DBN diagnosis models with different hyper-parameters have different diagnosis performance. With the change of the neuron numbers of hidden layers and the dropouts, the relationship between different layers will change accordingly. The orthogonal test results show the strength of interaction among different layers, thus partly reveal the internal mechanisms of DBN diagnosis models.

IV. SIMULATION EXPERIMENTS

The hyper-parameters of the DBN diagnosis model were selected as shown in Table 4. And the dataset produced in Section III was employed for model training and testing. To simulate real engine sensory signals in working environment, all input data are contaminated with measurement noise. The noise injection formula is shown in (6) [29].

$$x = x_0 + l\sigma \cdot rand \tag{6}$$

In (6), x_0 is the clean input parameter; l is the noise control factor, indicating the severity of the measurement noise, where $l = 0.02$, σ is the standard deviation of the training data; *rand* is the function used to produce a random number subject to normal distribution.

Fig. 10 shows the training results of the DBN model using the training dataset contaminated with measurement noises. The solid red line indicates the training accuracy. And the black dotted line indicates the loss during the training process, which is the mean squared error (MSE) between target labels and diagnosis results.

TABLE 3. Results of orthogonal tests and extreme difference analysis.

Test No.	Factor							Accuracy
	Pre-training learning rate	Fine-tuning learning rate	Number of hidden layer's neurons	Hidden layer number	Batch size	Dropout	Momentum	
1	1	1	1	4	1	1	1	0.6231
2	1	2	2	3	5	4	5	0.5216
3	1	3	3	2	4	2	3	0.8052
4	1	4	5	5	3	3	2	0.1121
5	1	5	4	1	2	5	4	0.6104
6	2	1	2	5	4	5	5	0.1340
7	2	2	3	1	3	1	3	0.9143
8	2	3	5	4	2	4	2	0.1340
9	2	4	4	3	1	2	4	0.9959
10	2	5	1	2	5	3	1	0.7268
11	3	1	3	3	2	3	4	0.6024
12	3	2	5	2	1	5	1	0.4752
13	3	3	4	5	5	1	5	0.1000
14	3	4	1	1	4	4	3	0.5432
15	3	5	2	4	3	2	2	0.1255
16	4	1	5	1	5	2	4	0.8417
17	4	2	4	4	4	3	1	0.1146
18	4	3	1	3	3	5	5	0.3192
19	4	4	2	2	2	1	3	0.2742
20	4	5	3	5	1	4	2	0.1000
21	5	1	4	2	3	4	5	0.6181
22	5	2	1	5	2	2	3	0.1000
23	5	3	2	1	1	3	2	0.7700
24	5	4	3	4	5	5	4	0.1024
25	5	5	5	3	4	1	1	0.4904
K1	2.6723	2.6853	2.3123	3.6796	2.9642	2.4020	1.9549	2.6723
K2	2.9050	2.1257	1.8253	2.3814	1.7210	2.8683	1.2416	2.9050
K3	1.8463	2.1284	2.5243	2.9295	2.0892	2.3259	2.6369	1.8463
K4	1.6497	1.4846	2.4390	1.0996	2.0874	1.9169	3.1528	1.6497
K5	2.0809	2.0531	2.0534	0.9365	2.2925	1.6412	1.6929	2.0809
k1	0.5345	0.5371	0.4625	0.7359	0.5928	0.4804	0.3910	0.5345
k2	0.5810	0.4251	0.3651	0.4763	0.3442	0.5737	0.2483	0.5810
k3	0.3693	0.4257	0.5049	0.5859	0.4178	0.4652	0.5274	0.3693
k4	0.3299	0.2969	0.4878	0.2199	0.4175	0.3834	0.6306	0.3299
k5	0.4162	0.4106	0.4107	0.1873	0.4585	0.3282	0.3386	0.4162
R	0.2511	0.2401	0.1398	0.5486	0.1754	0.2454	0.3822	0.2511

The formula for calculating the loss is shown in (7).

$$Loss = \frac{1}{N}\sum_{i=1}^{N}\sum_{j=1}^{6}(y_i^j - \hat{y}_i^j)^2 \tag{7}$$

In (7), y_i^j is the jth element of the diagnosis result of the ith sample, $\hat{y}_i^j$ the jth element of the target label of the ith sample, and N the number of samples.

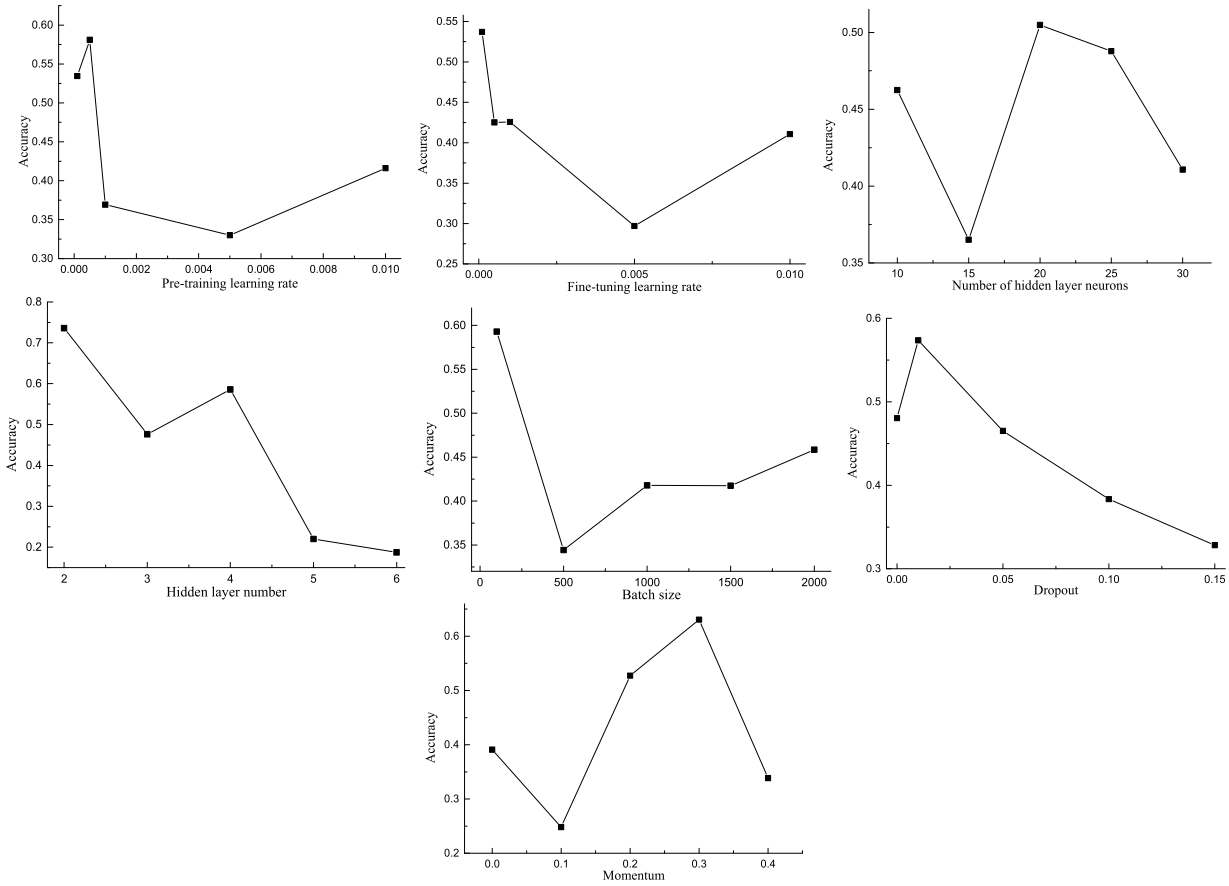

FIGURE 8. Trend chart of the orthogonal tests.

TABLE 4. The selected hyper-parameters.

Hyper-parameter	Value
Pre-training learning rate	0.0005
Fine-tuning learning rate	0.0001
Number of hidden layer neurons	20
Hidden layer number	2
Batch size	100
Dropout	0.01
Momentum	0.3

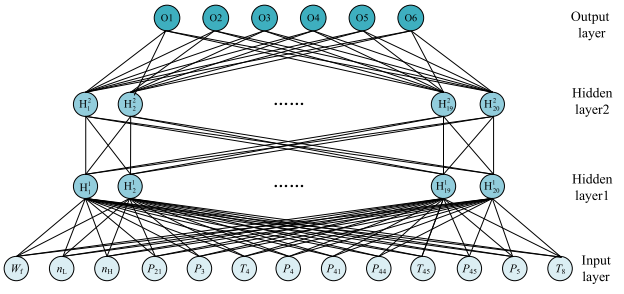

FIGURE 9. Structure of the optimized DBN model.

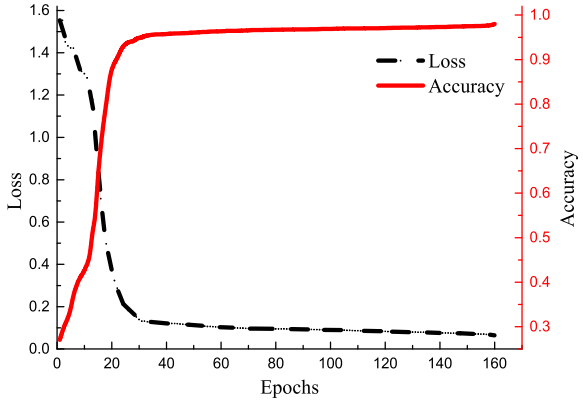

FIGURE 10. The training results of the DBN model.

It can be seen from Fig. 10 that the loss of the DBN model is rapidly falling during the training of the first 30 episodes, and a turning point appears when the loss approaches 0.1, after that the loss begins to decrease gradually. The change trend of the accuracy is almost the opposite of the change trend of the loss. After 30 episodes, the change of the accuracy becomes gentle, and the accuracy approaches 98%.

Fig. 11 shows the partial prediction results of a fault diagnosis test. Only 2 of the 34 randomly selected results are diagnosed wrong.

To further demonstrate and illustrate the performance of the DBN diagnosis model, it was compared with two other

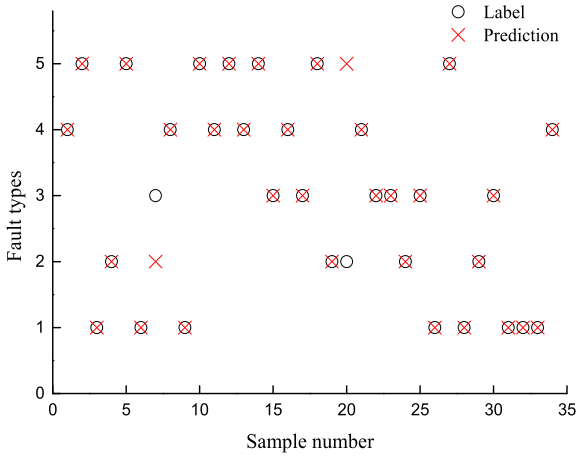

FIGURE 11. Partial prediction results of a fault diagnosis test.

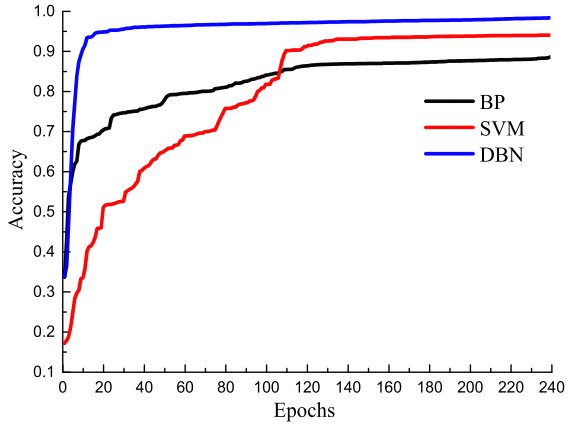

FIGURE 12. Comparison of the prediction results of the three diagnosis models.

AI diagnosis approaches, backpropagation neural network (BP) and support vector machine (SVM) [30]–[32]. BP neural network adopts the structure of single hidden layer, with the learning rate 0.01 and the hidden layer neuron number 20. SVM uses Gauss kernel function, the regularization factor C is 0.01, and the width of Gauss kernel γ is 0.001. The training results of the three models are shown in Fig. 11.

It can be seen from Fig. 12 that the accuracy of the DBN diagnosis model tends to be stable after about 40 training episodes. Although there are still some small fluctuations in the later stage of training, the accuracy is maintained around 98%. In contrast, the traditional BP network has the poorest diagnosis performance, and its accuracy is as low as 87%. The SVM accuracy is slightly higher than the BP network, but its convergence speed is slowest, and the required training episodes for convergence is much larger than DBN. Furthermore, the DBN's fluctuation range is also the smallest after convergence, which indirectly reflects the DBN model's robustness against external interference. Table 5 shows the average training accuracy and test accuracy of the three models. Apparently, the DBN model shows the best diagnosis performance.

TABLE 5. Average training and test accuracy of the three diagnosis models.

Model	Training accuracy（%）	Test accuracy（%）
BP	87.12%	86.05%
SVM	93.84%	91.76%
DBN	98.13%	96.59%

V. CONCLUSION

A DBN-based gas path fault diagnosis scheme for turbofan engines, which is composed of a turbofan engine reference model and a DBN diagnosis model, is proposed in this paper. The DBN diagnosis model is composed of several RBMs and was trained with the contrastive divergence algorithm and the back propagation algorithm. To optimize the performance of the DBN diagnosis model, the orthogonal tests were adopted to determine the hyper-parameters, such as learning rate, hidden layer number, hidden layer neuron number, etc. The DBN-based scheme proposed in this paper was applied to diagnose the gas path faults of a gas turbofan engine model and compared with BP-based and SVM-based schemes. The results show that the fault diagnosis accuracy of the DBN-based scheme is as high as 96.59%. Although the proposed scheme is designed for turbofan engines, it can also be used for fault diagnosis of other types of aero-engines through a little expansion.

REFERENCES

[1] R. Cheng and J. Y. Dan, "Missile turbofan engine fault diagnosis technology and its application," in *Foundations and Practical Applications of Cognitive Systems and Information Processing*. Berlin, Germany: Springer, 2014, doi: 10.1007/978-3-642-37835-5_65.

[2] P. Zhang and J.-Q. Huang, "Aeroengine fault diagnosis using dual Kalman filtering technique," *J. Aerosp. Power*, vol. 23, no. 5, pp. 952–956, May 2008.

[3] F. Lu, Y. Huang, J. Huang, and X. Qiu, "A hybrid Kalman filtering approach based on federated framework for gas turbine engine health monitoring," *IEEE Access*, vol. 6, pp. 9841–9853, 2017, doi: 10.1109/ACCESS.2017.2780278.

[4] J. Kraft, V. Sethi, and R. Singh, "Optimization of aero gas turbine maintenance using advanced simulation and diagnostic methods," *J. Eng. Gas Turbines Power*, vol. 136, no. 11, Nov. 2014, Art. no. 111601, doi: 10.1115/1.4027356.

[5] A. Aïtouche, F. Busson, B. O. Bouamama, and M. Staroswiecki, "Multiple sensor faults detection of steam condensers," *Comput. Chem. Eng.*, vol. 23, pp. S585–S588, Jun. 1999, doi: 10.1016/S0098-1354(99)80144-6.

[6] Y. Yuan, X. Liu, S. Ding, and B. Pan, "Fault detection and location system for diagnosis of multiple faults in aeroengines," *IEEE Access*, vol. 5, pp. 17671–17677, 2017, doi: 10.1109/ACCESS.2017.2744639.

[7] M. Zedda and R. Singh, "Fault diagnosis of a turbofan engine using neural networks—A quantitative approach," in *Proc. 34th AIAA/ASME/SAE/ASEE Joint Propuls. Conf. Exhib.*, Jul. 1998, p. 3602, doi: 10.2514/6.1998-3602.

[8] S. O. T. Ogaji and R. Singh, "Advanced engine diagnostics using artificial neural networks," in *Proc. IEEE Int. Conf. Artif. Intell. Syst.*, Sep. 2002, pp. 236–241, doi: 10.1109/ICAIS.2002.1048094.

[9] S. S. Tayarani-Bathaie, Z. N. S. Vanini, and K. Khorasani, "Dynamic neural network-based fault diagnosis of gas turbine engines," *Neurocomputing*, vol. 125, pp. 153–165, Feb. 2014, doi: 10.1016/j.neucom.2012.06.050.

[10] Y. LeCun, Y. Bengio, and G. Hinton, "Deep learning," *Nature*, vol. 521, pp. 436–444, May 2015, doi: 10.1038/nature14539.

[11] S. Khan and T. Yairi, "A review on the application of deep learning in system health management," *Mech. Syst. Signal Process.*, vol. 107, pp. 241–265, Jul. 2018, doi: 10.1016/j.ymssp.2017.11.024.

[12] R. Zhao, R. Yan, Z. Chen, K. Mao, P. Wang, and R. X. Gao, "Deep learning and its applications to machine health monitoring," *Mech. Syst. Signal Process.*, vol. 115, pp. 213–237, Jan. 2019, doi: 10.1016/j.ymssp.2018.05.050.
[13] P. Tamilselvan and P. F. Wang, "Failure diagnosis using deep belief learning based health state classification," *Rel. Eng., Syst. Safety*, vol. 115, pp. 124–135, Jul. 2013, doi: 10.1016/j.ress.2013.02.022.
[14] X. S. Lin, B. W. Li, and X. Y. Yang, "Engine components fault diagnosis using an improved method of deep belief networks," in *Proc. 7th Int. Conf. Mech. Aerosp. Eng. (ICMAE)*, Jul. 2016, pp. 454–459, doi: 10.1109/ICMAE.2016.7549583.
[15] B. Wang, R. Lin, D. Liu, J. Xu, and B. Feng, "Investigation of the effect of humidity at both electrode on the performance of PEMFC using orthogonal test method," *Int. J. Hydrogen Energy*, vol. 44, no. 26, pp. 13737–13743, May 2019, doi: 10.1016/j.ijhydene.2019.03.139.
[16] Z. Li and B. Yan, "Neural network parameter optimization and fault diagnosis based on orthogonal experiments," in *Proc. 8th World Congr. Intell. Control Automat.*, Jul. 2010, pp. 5800–5803, doi: 10.1109/WCICA.2010.5554612.
[17] D. J. Cai, Q. Shu, B. Q. Xu, L. M. Peng, and Y. He, "Orthogonal test design for optimization of the extraction of flavonid from the fructus gardeniae," *Biomed. Environ. Sci.*, vol. 24, no. 6, pp. 688–693, Dec. 2011, doi: 10.3967/0895-3988.2011.06.015.
[18] A. J. Volponi, "Gas turbine engine health management: Past, present, and future trends," *J. Eng. Gas Turbines Power*, vol. 136, no. 5, May 2014, Art. no. 051201, doi: 10.1115/1.4026126.
[19] D.-L. Feng, M.-Q. Xiao, Y.-X. Liu, H.-F. Song, Z. Yang, and Z.-W. Hu, "Finite-sensor fault-diagnosis simulation study of gas turbine engine using information entropy and deep belief networks," *Frontiers Inf. Technol. Electron. Eng.*, vol. 17, no. 12, pp. 1287–1304, Dec. 2016, doi: 10.1631/FITEE.1601365.
[20] R. Mohammadi, E. Naderi, K. Khorasani, and S. Hashtrudi-Zad, "Fault diagnosis of gas turbine engines by using dynamic neural networks," in *Proc. IEEE Int. Conf. Qual. Rel. (ICQR)*, Sep. 2011, pp. 25–30, doi: 10.1109/ICQR.2011.6031675.
[21] Z. Fan, C. Sun, and J. Bai, *Introduction to Aeroengine Fault Diagnosis*, 1st ed. Beijing, China: Science Press, 2004, pp. 4–5.
[22] G. Hinton, "A practical guide to training restricted Boltzmann machines," in *Neural Networks: Tricks of the Trade* (Lecture Notes in Computer Science), vol. 7700, 2nd ed. Berlin, Germany: Springer-Verlag, 2012, pp. 599–619, doi: 10.1007/978-3-642-35289-8_32.
[23] W. Jing, T. Jiang, and Y. Liu, "An optimization of DBN/GPU speech recognition on wireless network applications," in *Proc. Int. Wireless Internet Conf. (WICON)*, Dec. 2017, pp. 189–196, doi: 10.1007/978-3-319-72998-5_20.
[24] L. L. Lin, H. J. Dong, and X. Y. Song, "DBN-based classification of spatial-spectral hyperspectral data," in *Advances in Intelligent Information Hiding and Multimedia Signal Processing*, vol. 64. Taiwan, China, 2017, pp. 53–60, doi: 10.1007/978-3-319-50212-0_7.
[25] J. Chen, S. Cheng, H. Xie, L. Wang, and T. Xiang, "Equivalence of restricted Boltzmann machines and tensor network states," Jan. 2017, *arXiv:1701.04831*. [Online]. Available: https://arxiv.org/abs/1701.04831
[26] P. Mamoshina, A. Vieira, E. Putin, and A. Zhavoronkov, "Applications of deep learning in biomedicine," *Mol. Pharmaceutics*, vol. 13, no. 5, pp. 1445–1454, 2016, doi: 10.1021/acs.molpharmaceut.5b00982.
[27] R. Merzouki, A. K. Samantaray, P. M. Pathak, and B. O. Bouamama, "Model-based fault diagnosis and fault tolerant control," in *Intelligent Mechatronic Systems*, Nov. 2012, pp. 577–617, doi: 10.1007/978-1-4471-4628-5_7.
[28] M. Li and R. Guo, "The optimal Mars entry guidance with external disturbance using neural network solution," in *Proc. Chin. Intell. Automat. Conf.*, 2019, pp. 521–528, doi: 10.1007/978-981-32-9050-1_59.
[29] W. Yu, Z. Ma, A. S. H. Lau, and X. Huang, "Analysis and experiment of the compressive sensing approach for duct mode detection," *AIAA J.*, vol. 56, no. 2, pp. 648–657, Dec. 2017, doi: 10.2514/1.J056347.
[30] C. Vununu, K.-R. Kwon, E.-J. Lee, K.-S. Moon, and S.-H. Lee, "Automatic fault diagnosis of drills using artificial neural networks," in *Proc. IEEE ICMLA*, Dec. 2017, pp. 992–995, doi: 10.1109/ICMLA.2017.00-23.
[31] C.-C. Hsu, M.-C. Chen, and L.-S. Chen, "Intelligent ICA–SVM fault detector for non-Gaussian multivariate process monitoring," *Expert Syst. Appl.*, vol. 37, no. 4, pp. 3264–3273, Apr. 2010, doi: 10.1016/j.eswa.2009.09.053.
[32] X. Y. Jin, S. S. Zhong, G. Ding, and L. Lin, "Engine testing fault classification based on the multi-class SVM of auto-regression," in *Advances in Information Technology and Industry Applications*, Jan. 2012, pp. 33–38, doi: 10.1007/978-3-642-26001-8_5.

JIANGUO XU was born in Jincheng, China, in 1971. He received the B.S. degree in thermal power machinery and equipment from Beijing Jiaotong University, Beijing, China, in 1993, and the Ph.D. degree in mechanical manufacturing and automation from the Nanjing University of Technology, Nanjing, China, in 2007.

Since 2007, he has been a Lecturer with the College of Energy and Power Engineering, Nanjing University of Aeronautics and Astronautics. His current research interests include the fields of AI-based fault diagnosis and control for aero-engines and embedded system design.

XINGYI LIU received the B.S. degree in mechanical engineering from Nanhang Jincheng College, Nanjing, China, in 2017. He is currently pursuing the master's degree with the College of Energy and Power Engineering, Nanjing University of Aeronautics and Astronautics, Nanjing. His main research interest includes intelligent fault diagnosis for aero-engines.

BINBIN WANG received the B.S. degree in energy and power engineering from the Henan University of Science and Technology, China, in 2018. He is currently pursuing the master's degree with the College of Energy and Power Engineering, Nanjing University of Aeronautics and Astronautics, Nanjing, China. His main research interest includes intelligent fault diagnosis for aero-engines.

JIAQI LIN received the B.S. and M.S. degrees in aerospace propulsion theory and engineering from the Nanjing University of Aeronautics and Astronautics, Nanjing, China, in 2015 and 2018, respectively. He has been with China Mobile (Suzhou) Software Technology Company Ltd., as an Engineer, since 2018. His current research interest includes intelligent fault diagnosis for aero-engines and data mining.